

Combined Effect of Spin Speed and Ionic Strength on Polyelectrolyte Spin Assembly

Pritesh A. Patel,[†] Andrey V. Dobrynin,^{‡,§} and Patrick T. Mather^{*,†,||}

Department of Macromolecular Science and Engineering, Case Western Reserve University, Cleveland, Ohio 44106, Polymer Program, Institute of Materials Science, and Department of Physics, University of Connecticut, Storrs, Connecticut 06269

Received July 10, 2007. In Final Form: August 21, 2007

Polyelectrolyte spin assembly (PSA) of multilayers is a sequential process featuring adsorption of oppositely charged polyelectrolytes from dilute solutions undergoing spin-coating flow. Here, we report on the dependence of PSA multilayer buildup of poly(sodium 4-styrenesulfonate) and poly(allylamine hydrochloride) on solution ionic strength and spin speed. We observed that at a given spin speed, the PSA coating growth rate (thickness/bilayer) and polymer surface coverage shows a nonmonotonic dependence on salt concentration, first increasing and then decreasing with increasing solution ionic strength. This is argued to be a manifestation of two competing mechanisms responsible for the layer formation. At low salt concentrations, the electrostatic interactions control the multilayer assembly process, while at high salt concentrations it is dominated by shear flow. We explain this nonmonotonic behavior in the framework of a Flory-like theory of multilayer formation from polyelectrolyte solution under shear flow. Additionally, the PSA process led to multilayer coatings with a radial dependence on thickness at lower spin speed in the shear-dominated regime. On increasing spin speed, such radial dependence subsided, eventually leading to uniform coatings by planarization. The surface topography of the multilayered coatings adsorbed at salt concentration less than 0.1 M was flat and featureless for all studied spin speeds. Unique morphological features in the films were formed at salt concentration higher than 0.1 M, the size of which depended on the spin speed and solution ionic strength.

Introduction

Layer-by-layer (LbL) assembly of polyelectrolytes on surfaces has become a simple and versatile technique to produce multilayered, multicomponent thin films, and the method has been the subject of numerous reviews.^{1–7} Usually, such multilayered films are made by alternating immersion (“dipping”) of a charged substrate into aqueous polyelectrolyte solutions of opposite (i.e., positive/negative) charge with a rinse step in between every deposition step. This process is repeated multiple times to achieve film growth until the desired thickness or number of “bilayers”. Here, a bilayer consists of an alternating deposition of polyanion and polycation with an intervening rinse step. The key to sustained growth of a coating by the LbL process is charge inversion and subsequent reconstruction of the surface properties after each deposition step. Experiments have shown a stepwise increase of multilayer thickness or film mass, or surface coverage with each deposition cycle—hereby, referred as growth rate—indicating a steady-state regime after each deposition step.^{8–10}

Typically, the thickness increment has been shown to be around 10–60 Å per bilayer or deposition cycle. The thickness of the multilayers assembled by the dipping LbL process is controlled by solution pH, ionic strength, charge fraction of polyelectrolyte (ionization), and solvent quality.⁹ It has also been established by simulations^{11,12} that electrostatic and short-range interactions play an important role in the LbL assembly process and that for the total charges adsorbed during the deposition of a new layer, approximately 50% of those charges neutralize the oppositely charged substrate while the remaining 50% overcompensate (or “overcharge”) the substrate. The latter is consistent with LbL growth at steady state. The simplicity of this technique, with practically no limitations on the shape of the charge-bearing substrate or polyelectrolyte pair, has opened up applications in a wide variety of areas, including biosensors,¹³ biology and medicine,¹⁴ light-emitting systems,¹⁵ electroanalytical chemistry,¹⁶ selective area patterning,⁶ drug delivery,¹⁷ free-standing films,¹⁸ and biomineralization,¹⁹ among many others.

Despite such advantages, dipping-based LbL for multilayer film assembly is a very time-consuming process lasting hours, with each dipping step requiring between 10 and 30 min for the deposition. As an alternative, spin-assisted LbL assembly allows rapid processing of the multilayered films by employing

* Corresponding author. E-mail: ptmather@syr.edu.

[†] Case Western Reserve University.

[‡] Polymer Program, Institute of Materials Science, University of Connecticut.

[§] Department of Physics, University of Connecticut.

^{||} Present address: Department of Biomedical and Chemical Engineering, Syracuse University.

(1) Decher, G.; Schlenoff, J. B. *Multilayer Thin Films: Sequential Assembly of Nanocomposite Materials*; Wiley-VCH: Verlag, 2002.

(2) Decher, G. *Science* **1997**, *277* (5330), 1232–1237.

(3) Decher, G.; Hong, J. D. *Makromole. Chem., Macromol. Symp.* **1991**, *46*, 321–327.

(4) Decher, G.; Hong, J. D. *Ber. Bunsen-Ges.* **1991**, *95* (11), 1430–1434.

(5) Decher, G. Multilayer films (polyelectrolytes). In *The Polymeric Materials Encyclopedia: Synthesis, Properties and Applications*; Slasmore, J. C., Ed.; CRC Press: Boca Raton, FL, 1996.

(6) Hammond, P. T. *Adv. Mater.* **2004**, *16* (15), 1271–1293.

(7) Zhang, X.; Chen, H.; Zhang, H. *Chem. Comm.* **2007**, *14*, 1395–1405.

(8) Decher, G.; Lvov, Y.; Schmitt, J. *Thin Solid Films* **1994**, *244*, 772–777.

(9) Dubas, S. T.; Schlenoff, J. B. *Macromolecules* **1999**, *32*, 8153–8160.

(10) Schlenoff, J. B.; Ly, H.; Li, M. *J. Am. Chem. Soc.* **1998**, *120*, 7626–7634.

(11) Patel, P. A.; Jeon, J.; Mather, P. T.; Dobrynin, A. V. *Langmuir* **2005**, *21* (13), 6113–6122.

(12) Patel, P. A.; Jeon, J.; Mather, P. T.; Dobrynin, A. V. *Langmuir* **2006**, *22* (24), 9994–10002.

(13) Zhao, W.; Xu, J.-J.; Chen, H.-Y. *Electroanalysis* **2006**, *18* (18), 1737–1748.

(14) Haynie, D. T.; Zhang, L.; Zhao, W.; Rudra, J. S. *Nanomedicine* **2006**, *2* (3), 150–157.

(15) Fou, A. C.; Onitsuka, O.; Ferreira, M.; Rubner, M. F. *J. Appl. Phys.* **1996**, *79*, 7501–7509.

(16) Zheng, L.; Yao, X.; Li, J. *Curr. Anal. Chem.* **2006**, *2* (3), 279–296.

(17) Sukhishvili, S. A. *Curr. Opin. Colloid Interface Sci.* **2005**, *10* (1,2), 37–44.

(18) Jiang, C.; Tsukruk, V. V. *Adv. Mater.* **2006**, *18* (7), 829–840.

(19) Ngankam, P. A.; Lavallo, P.; Voegelé, J. C.; Szyk, L.; Decher, G.; Schaaf, P.; Cuisinier, F. J. G. *J. Am. Chem. Soc.* **2000**, *122* (37), 8998–9005.

conventional spin-coating methods.^{20–27} With this technique, a spin coater is used to adsorb the polyelectrolyte layers onto a charged substrate by applying excess polyelectrolyte solution before or during the spinning, followed by a rinsing by exposure of the same spinning substrate to pure water. During the spinning, most of the (excess) solution is expelled out (< 1 s) due to centrifugal forces, leaving a film with thickness $\sim 1 \mu\text{m}$, following which the solution coating more gradually thins and dries over the course of 2–15 s. The whole deposition process of a single polyelectrolyte layer usually takes about 10–15 s compared to the conventional 10–30 min for the quiescent adsorption (“dipping”). This spin assembly (SA), or polyelectrolyte spin assembly (PSA), has been shown to produce more compact and less intermixed layers with lower roughness compared to the films produced by the dipping process.²⁰ Due to the faster processing time afforded by PSA, free-standing films have easily been made for a wide variety of applications.^{18,28} This method has been applied to build multilayered films consisting of synthetic polyelectrolytes,²⁰ nanoparticles,²⁹ dendrimers,²¹ dye molecules,³⁰ and surfactants,³¹ among other charged species.

The mechanism of the polyelectrolyte adsorption for PSA is different than the diffusion-controlled adsorption of the polyelectrolytes in the dipping technique. For the PSA case, the combination of the shear stress due to flow and electrostatic interactions between polyelectrolytes are the dominant factors controlling the film structure. Several studies have reported the effect of parameters like polyelectrolyte molecular weight,²³ concentration,^{21,24} and spin speed^{23,25,27} on the growth rate of the multilayers formed by PSA. In series of papers,^{23,25,27,32} Lee and Cho have studied the effect of such parameters on the growth of multilayers by PSA. They observed that the growth rate depends weakly (logarithmically) on the polyelectrolyte molecular weight, with higher molecular weight polyelectrolytes showing lower growth rate.²³ These findings were attributed to the denser packing afforded by the low molecular weight as compared to the high molecular weight polyelectrolytes. The same group reported that the growth rate of the multilayers by PSA first increased with polyelectrolyte concentration up to 10 mM (based on repeat unit molar mass) and then reached a constant value with no further dependence at higher polyelectrolyte concentration. In contrast, the multilayer growth rate by PSA decreases with increasing the spin speed, as reported in various studies.^{23,25,27} Such PSA growth rate (absorbance per bilayer, Γ) dependence was fitted to an empirical power-law function that consisted of two terms: polyelectrolyte concentration (cp) and spin speed (ω) ($\Gamma \sim \omega^\alpha c_p^\beta$).²⁵ The power-law exponent for polyelectrolyte concentration, β , was 0.78 for the concentration range of 1–10 mM. On other hand, the power-law exponent of spin speed, α ,

was -0.34 , a smaller (negative) value compared to that obtained for the conventional spin-coating of noncharged polymer solutions (usually, -0.5). This lower spin speed exponent was attributed to the effect of strong electrostatic force observed by the polyelectrolyte during the spin-coating flow, but no fundamental explanation has been given.

In contrast to the effect of polymer concentration, molecular weight, and spin speed, salt concentration has a strong effect on the multilayer buildup by PSA. For PSA assembly from polyelectrolyte solutions with no salt, the growth rate of the multilayer coatings by spin assembly is higher than the dipping technique.²⁰ Such a trend in the growth rate of multilayers is reversed on addition of salt to polyelectrolyte solutions. Cho et al.,³³ while studying the multilayer growth by PSA on patterned surfaces, had found that the growth rate of multilayers by PSA is lower than that deposited by dipping assembly on salt addition in the range of 0.1–1.0 M NaCl. They attributed this to strong desorption forces, specifically centrifugal and shear force, that led to a pronounced effect of added salt on the polyelectrolyte conformation. However, no fundamental explanation or empirical relation for the dependence of growth rate on spin speed and salt concentration was suggested. Additionally, the same researchers have found that well-defined pattern shapes (“pattern quality”) were obtained at an intermediate ionic strength of 0.4 M using PSA. Lefaux et al.,²⁶ using UV–vis spectroscopy and AFM, studied the dependence of the multilayer growth rate on the solution ionic strength at fixed spin speed of 3000 rpm. It was found that the growth rate of polymer surface coverage and thickness increased rapidly with salt concentration up to 0.1 M and then reached a constant value at higher ionic strengths. These experimental results were analyzed within the framework of the Flory-like model of the multilayer assembly, which accounts for both the effect of the electrostatic interactions between oppositely charged chains within multilayers and chain deformation by shear flow. At steady-state multilayer growth, the model predicts that the growth rate of polymer surface coverage per bilayer, Γ , can be described by the following equation²⁶

$$\Gamma \approx \alpha \frac{c^{-1/2}}{c^{-1} + \beta \dot{\gamma}^{2/3}} \quad (1)$$

where α and β are fitting parameters, $\dot{\gamma}$ is the shear rate, and c is the salt concentration of the solution, including both added salt and polyelectrolyte counterions. Equation 1 predicts two regimes of multilayer buildup by PSA: (i) at low salt concentration, the c^{-1} term dominates over the shear rate term (in the denominator), predicting square root dependence of surface coverage on salt concentration, $\Gamma \propto c^{1/2}$, and (ii) at high salt concentration, shear rate term dominates, predicting inverse square root dependence of surface coverage, $\Gamma \propto c^{-1/2}$. The equation agreed reasonably well with experimental data of PSA at 3000 rpm.²⁶ However, the experimental data of the growth rate measured at the disk center for PSA process at this spin speed did not reveal the second regime of decreasing growth rate with salt concentration, as predicted by eq 1. As we will show, this was due to the parameters of the previous study²⁶ that focused on PSA near the disk center (~ 1 mm) and a relatively low spin speed of 3000 rpm.

In this paper, we extend the previous study²⁶ to consider the combined effects of both the PSA spin speed and salt concentration on coating growth rate, morphology, thickness, and roughness of multilayer coatings. Extending the range of spin speeds and disk radii explored, we found, for the first time, that increasing

(20) Cho, J.; Char, K.; Hong, J.-D.; Lee, K.-B. *Adv. Mater.* **2001**, *13* (14), 1076–1078.

(21) Chiarelli, P. A.; Johal, M. S.; Casson, J. L.; Roberts, J. B.; Robinson, J. M.; Wang, H.-L. *Adv. Mater.* **2001**, *13* (15), 1167–1171.

(22) Chiarelli, P. A.; Johal, M. S.; Holmes, D. J.; Casson, J. L.; Robinson, J. M.; Wang, H.-L. *Langmuir* **2002**, *18* (1), 168–173.

(23) Lee, S.-S.; Lee, K.-B.; Hong, J.-D. *Langmuir* **2003**, *19* (18), 7592–7596.

(24) An, M.; Hong, J.-D. *Thin Solid Films* **2006**, *500* (1–2), 74–77.

(25) Cho, J.; Lee, S.-H.; Kang, H.; Char, K.; Koo, J.; Seung, B. H.; Lee, K.-B. *Polymer* **2003**, *44* (18), 5455–5459.

(26) Lefaux, C. J.; Zimberlin, J. A.; Dobrynin, A. V.; Mather, P. T. *J. Polym. Sci., Part B: Polym. Phys.* **2004**, *42* (19), 3654–3666.

(27) Lee, S.-S.; Hong, J.-D.; Kim, C. H.; Kim, K.; Koo, J. P.; Lee, K.-B. *Macromolecules* **2001**, *34* (16), 5358–5360.

(28) Jiang, C.; Markutsya, S.; Tsukruk, V. V. *Adv. Mater.* **2004**, *16* (2), 157–161.

(29) Sohn, B.-H.; Kim, T.-H.; Char, K. *Langmuir* **2002**, *18* (21), 7770–7772.

(30) Campbell, V. E.; Chiarelli, P. A.; Kaur, S.; Johal, M. S. *Chem. Mater.* **2005**, *17* (1), 186–190.

(31) Joha, M. S.; Chiarelli, P. A. *Soft Matter* **2006**, *3* (1), 34–46.

(32) Fou, A. C.; Onitsuka, O.; Ferreira, M.; Rubner, M. F.; Hsieh, B. R. *J. Appl. Phys.* **1996**, *79* (10), 7501–7509.

(33) Cho, J.; Jang, H.; Yeom, B.; Kim, H.; Kim, R.; Kim, S.; Char, K.; Caruso, F. *Langmuir* **2006**, *22* (3), 1356–1364.

ionic strength actually results in a decrease in the growth rate of the multilayers at higher spin speed and/or higher radial distance, each corresponding to an increased shear rate. Favorable agreement with a Flory-like theory of multilayer formation from polyelectrolyte solution under shear flow, taking into account the effects of shear rate and ionic strength, will be shown to provide insight into the fundamentals of polyelectrolyte adsorption under the shear flow. The rest of the paper is organized as follows: experimental procedures are discussed in section 2 and results and discussion are presented in section 3, followed by our conclusions in section 4.

Experimental Section

Preparation of Multilayers. Quartz (1" diameter \times 1/16" thick) discs (Chemglass) were used as the substrates for preparation of multilayered coatings by polyelectrolyte spin assembly. Substrates were treated with piranha solution (70:30 v/v H₂SO₄:H₂O₂) at 60 °C for 1 h, followed by sonication for 5 min (**Caution:** Piranha solution is extremely corrosive, and special care must be taken during handling of such a solution). Substrates were then rinsed multiple times in ultrapure deionized (DI) water (Milli-Q, $\rho > 18$ M Ω cm) and dried. To produce a charged surface primed for polyelectrolyte adsorption, a layer of low molecular weight poly(ethyleneimine) (PEI) (Aldrich, CAS No. 025987068) (3 wt % solution in DI water) was deposited on the substrate by spin coating at 5000 rpm for a duration of 15 s (Laurell Technologies Corp., Model WS-400B-6NPP/LITE). Such a substrate was then rinsed with DI water three times under the same spinning conditions to remove the loosely adsorbed PEI and obtain a uniform layer of the positive charge on the substrate. It was found that the multiple rinsing steps with DI water are necessary to remove the loosely adsorbed PEI from the substrate, since this irreproducibly affects the initial growth rate of the LbL assembly before the steady growth rate is achieved. For the growth of multilayers using PSA, poly(sodium 4-styrenesulfonate) (PSS) ($M_w = 70$ kDa) (Aldrich) was used as polyanion and poly(allylamine hydrochloride) (PAH) ($M_w = 15$ kDa) (Aldrich) was used as polycation. The concentration of both polyelectrolyte solutions was 0.01 M based on the molar mass of each repeat unit of polymer (206 and 93.5 g/mol for PSS and PAH, respectively). Noting that the pK_a values for PSS and PAH are ca. 1.0³⁴ and 8.5, respectively, the pH of each polyelectrolyte solution was adjusted to 3.5 using 0.1 M HCl. Thus, both solutions will contain polyelectrolytes that are nearly fully charged.²⁶ The ionic strength of the polyelectrolyte solution (0.01 M) was varied by adding NaCl to different concentration levels between 0 M (no salt) and 1.0 M. In the text, we refer to different solutions based on their NaCl concentration; however, it is worth noting that the total ionic strength of the polyelectrolyte solutions includes both the counterion concentration of the polyelectrolytes (10⁻² M) and the added salt.

Multilayer coatings by PSA on quartz substrate were made for each combination of the spin speeds (3000, 5000, and 6000 rpm) and salt concentrations (0, 0.05, 0.1, 0.25, 0.5, and 1.0 M) using polyelectrolyte (PSS or PAH) concentration at 10⁻² M. Multilayers were constructed by following the procedure reported previously.²⁶ Briefly, the deposition process for each cycle, or bilayer, was performed as follows: (1) several drops of PSS solution are placed on the quartz substrate to completely cover the surface followed by spinning at a prescribed spin speed for 15 s, (2) two washing steps with DI water are accomplished using the same sequence as during step 1, (3) step 1 is repeated with PAH polyelectrolyte solution, and (4) washing steps with DI water similar to step 2 are repeated. These steps were repeated multiple times until the prescribed number of deposition cycles was reached. We note that in our experimental procedure, the polyelectrolyte solutions were first deposited on substrate before spinning, in contrast to some reports³⁵ where the

solution was deposited on to the already spinning substrate. This was done to ensure that the surface is entirely covered with excess polyelectrolyte solution before spinning the substrate. The delay between the solution deposition on the substrate and the spinning of substrate in our case was typically 2–3 s. We are confident that such short delay would not result in any adsorption similar to the quiescent case, since for the latter case the deposition generally requires 10–20 min to reach equilibrium adsorption.

Characterization. Film growth by PSA on quartz substrates was monitored by measuring the increasing absorbance intensity of the distinct π to π^* transition of PSS at 226 nm with UV–vis spectrometry (Varian Cary 50 UV–vis spectrophotometer). A clean quartz disk with the same thickness was used as a reference for the spectra, while the UV–vis absorbance spectra were taken every two or four cycles of consecutive deposition of PSS and PAH with a rinse step in between. In contrast to PSS, PAH shows no detectable features in the UV–vis spectrum (190–700 nm). Spatially, the UV–vis spectrometer allowed measurements of the amount of PSS (surface coverage) within the spot of the beam with diameter of 1 mm on the substrate. This feature was exploited to examine the potential radial dependence of coating thickness. Thus, spectra were taken at precise radial positions of each disc after first aligning the beam to the disk center and then displacing the disc using a custom-built linear translation stage. The growth rates of the multilayered coatings are reported from the PSS absorbance taken at 6 mm from the disc center, unless otherwise noted. The arrangement also allowed measurements of multilayer growth rate at different radial positions on each substrate. The radial dependence of the UV absorbance, each value being a measure of the amount of polymer adsorbed, was investigated after deposition of 20 bilayers of the PSS and PAH for each combination of the spin rate and solution ionic strength at constant polyelectrolyte concentration.

Atomic Force Microscopy (AFM). Surface morphology, roughness, and thickness measurements of multilayers were obtained from the height images collected using contact-mode atomic force microscopy (AFM) (Veeco Digital Instruments Dimension 3100 scanning probe microscope). Measurements were performed on the multilayered coatings on the quartz after deposition of 32 bilayers for each set of spin speed and salt concentrations. Contact mode-AFM can noninvasively probe multilayer surface morphology,^{26,36} owing to the high modulus and toughness of such coatings in the dry state.^{37,38} The surface roughness was quantified from the AFM images using the imaging software (Veeco Instruments NanoScope II) that calculates the surface roughness by the following equation

$$R_a = \sqrt{\frac{1}{N} \sum_{i=1}^N (h_i - \bar{h})^2} \quad (2)$$

where R_a is the root-mean-square roughness, h_i is the height value of each pixel, \bar{h} is the average height of all the pixels, and N is number of pixels in the scan area. It is known that roughness measurements depend on several factors, such as scan size, image bow or sample tilt, and other correction procedures for tip convolution effects on the acquired image.³⁹ In these studies, all the images were corrected for bow/tilt using a first-order flatten function in the image software before the roughness measurements were analyzed. AFM images were taken as 10 μ m \times 10 μ m scans on the multilayer film on quartz substrate, and roughness calculations were then performed over 5 μ m \times 5 μ m areas of the scan. The roughness values were averaged over six randomly selected areas covering the whole image. The same AFM tip and image processing algorithm were used for all of the measurements to allow fair comparison of roughness values across all samples.

(36) Menchaca, J. L.; Jachimska, B.; Cuisinier, F.; Perez, E. *Colloids Surf., A* **2003**, 222 (1–3), 185–194.

(37) Richert, L.; Engler, A. J.; Discher, D. E.; Picart, C. *Biomacromolecules* **2004**, 5 (5), 1908–1916.

(38) Picart, C.; Senger, B.; Sengupta, K.; Dubreuil, F.; Fery, A. *Colloids Surf., A* **2007**, 303 (1–2), 30–36.

(39) Kiely, J. D.; Bonnell, D. A. *J. Vac. Sci. Technol. B* **1997**, 15 (4), 1483–1493.

(34) Lvov, Y.; Price, R.; Gaber, B.; Ichinose, I. *Colloids Surf., A* **2002**, 198–200, 375–382.

(35) Jhal, M. S.; Casson, J. L.; Chiarelli, P. A.; Liu, D.-G.; Shaw, J. A.; Robinson, J. M.; Wang, H.-L. *Langmuir* **2003**, 19 (21), 8876–8881.

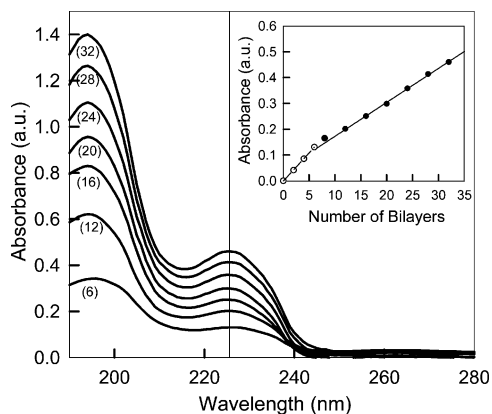


Figure 1. Absorbance versus wavelength for PSS/PAH (10^{-2} M, pH 3.5) films deposited by PSA using a salt concentration of 0.05 M and spin speed of 5000 rpm for different number of bilayers, shown in parentheses. The inset shows absorbance ($\lambda_{\text{max}} = 226$ nm) intensity versus number of bilayers for the same assembly. The solid line is a linear regression of the data set after the 10th bilayer (closed circles) and the dashed line is the regression of the data up to the eighth bilayer (open circles).

AFM-based thickness measurements were performed by first etching a portion of the film using the sharp edge of a razor blade that penetrates to the quartz substrate (but no further).²⁶ AFM scans of $50 \mu\text{m} \times 50 \mu\text{m}$ were performed on a region including the bare quartz, and the thickness was determined by the average height difference between the areas with and without the multilayered coatings.

Results and Discussion

The growth rate of the multilayer film deposited by the PSA technique was followed by growth of the PSS absorbance peak at 226 nm using UV-vis spectroscopy. Figure 1 shows the representative evolution of the absorbance spectra for PSS/PAH multilayers deposited at a salt concentration of 0.05 M and a spin rate of 5000 rpm with increasing deposition cycle number. Each absorbance spectrum was measured at a distance of 6 mm from the center of the disc in order to elucidate the effect of shear rate. The absorbance value (the peak amplitude) at 226 nm (Figure 1, inset) shows a linear growth after completion of eight deposition cycles. For the first few layers the absorbance values have different initial slope compared to the later stage of steady-state regime. This is consistent with prior studies, which have revealed that a steady-state linear growth regime is usually observed in the experiments after completion of the first few deposition cycles for the case of dipping assembly⁴⁰ and PSA.²² The growth rate difference at early stages—in this case a higher growth rate—is believed to result from the difference in surface charge density of the substrate compared to the natural overcharging at the steady-state regime.

Overcharging—that is, the overcompensation of surface charge by ca. 50% during adsorption of oppositely charged polyelectrolyte—is observed for steady-state growth as reported for PSA²² and from simulations.^{11,41} In experiments, this difference in growth rate has been observed for deposition from two to 16 deposition steps, depending on the substrate and the polyelectrolyte pairs.^{22,40} Nevertheless, after the linear (regular) growth regime is achieved, the slope does not change for subsequent deposition cycles, even for 50 deposition cycles at 5000 rpm from polyelectrolyte solutions with 0.1 M salt concentration (see Supporting Information, Figure S1). In order to study the linear steady-state growth rate of the

multilayer buildup for each experiment, we have followed the growth process by completing up to 32 deposition cycles. The steady-state growth rate was measured for each sample by linear regression of the absorbance values between the 10th and 32nd deposition steps. This allows comparison of the amount of polyelectrolyte adsorbed (or surface coverage) per deposition cycle at steady-state for a range of spin rates and salt concentrations for the PSA process. Previously, it has been shown that the linear growth of the adsorbed amount of PSS measured by UV-vis spectrometry was consistent with the thickness growth measurements obtained by AFM²⁶ and ellipsometry²² for the same polyelectrolyte pair deposited at 3000 rpm.

First, we consider the impact of added salt on PSA growth rate for several spin speeds. Figure 2 shows the growth of polymer surface coverage with the number of bilayers at different salt concentrations for PSS/PAH films spin assembled at (a) 3000 rpm, (b) 5000 rpm, and (c) 6000 rpm. The curves follow a similar linear growth pattern as seen previously in Figure 1 (inset), where a linear increase in the polymer surface coverage with the number of deposition cycles was observed after the completion of eight deposition cycles or bilayers. The difference in the initial slopes of all the curves is attributed to the difference between the initial surface charge and the overcharging achieved after each deposition at given conditions of spin speed and salt concentration, as was pointed out earlier. The different initial absorbance growth rate compared to the steady-state growth rate is further evidenced by the nonzero y-intercepts of the regression lines shown in Figure 2. Unlike the initial growth rate, which depends on the primer layer, the growth rates at the later stage signifies the effect of deposition conditions and are reproducible for each set of deposition conditions. In all cases, we have observed a linear increase in polymer surface coverage with the number of deposition cycles after several initial deposition cycles, as seen in Figure 2.

The growth rate of the multilayer coatings in the linear steady-state regime shows a nonmonotonic dependence on the salt concentration at a given spin rate. Figure 3 shows such behavior in the absorbance growth rate for the range of the salt concentrations and spin rate. Here, the growth rate was taken as the slope at steady state (late stage) for data sets shown in Figure 2. We see that the growth rate first increases rapidly with salt concentration for $c < 0.1$ M, reaches a peak near 0.25 M salt concentration, and then decreases. The rapid increase in the growth rate at low salt concentrations is quite similar for all spin rates studied. However, the salt concentration dependence of the growth rate at higher salt concentrations—the decreasing regime—shows strong dependence on the spin speed. In this salt concentration regime, the growth rate decreases faster for the multilayers built at higher spin speeds. The observed trend in the dependence of growth rate indeed follows the predicted form for polymer surface coverage given by eq 1 (in which the salt concentration, c , should include both the concentration of added salt and concentration of polyelectrolyte counterions).

Indeed, our observation confirms the existence of two competing mechanisms for the multilayer buildup process using PSA: a low salt regime of increasing growth rate and a high salt regime of decreasing growth rate. In the first regime, at low salt concentrations, $c < 0.1$ M, the adsorption of polyelectrolytes is controlled by electrostatic interactions between charged chains. The multilayer assembly in this salt concentration regime is similar to the quiescent LbL assembly. It is known that for dipping (quiescent) LbL assembly, the multilayer growth rate steadily increases with salt concentration. Dubas and Schlenoff⁹ have shown that for the dipping LbL assembly the growth rate varies

(40) Schlenoff, J. B.; Dubas, S. T. *Macromolecules* **2001**, *34* (3), 592–598.

(41) Jeon, J.; Panchagnula, V.; Pan, J.; Dobrynin, A. V. *Langmuir* **2006**, *22* (10), 4629–4637.

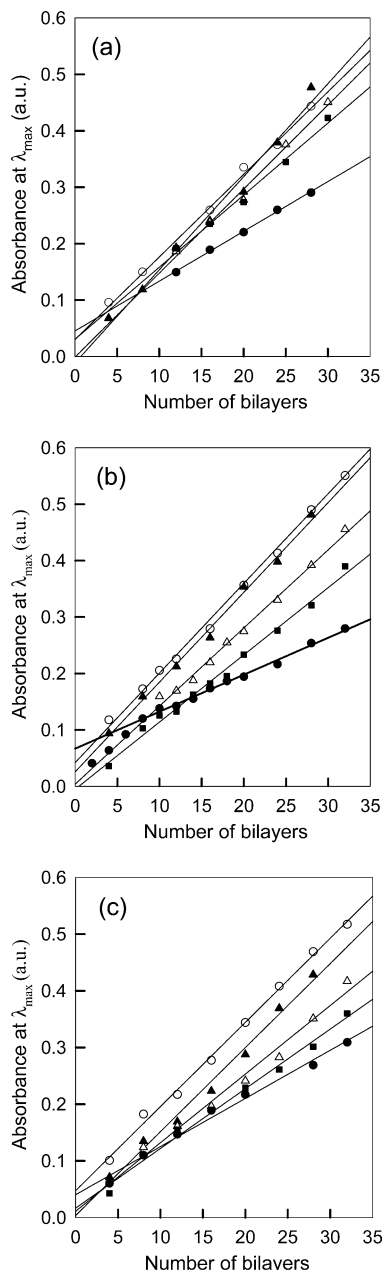


Figure 2. Dependence of the absorbance at λ_{\max} (226 nm) on the number of deposition cycles for PSS/PAH solutions ($c_p = 10^{-2}$ M, pH 3.5) at spin speeds of (a) 3000 rpm, (b) 5000 rpm, and (c) 6000 rpm and salt concentration of 0 M (closed circles), 0.1 M (open circle), 0.25 M (closed triangle), 0.5 M (open triangle), and 1 M (square). The UV-vis absorbance is measured at 6 mm from the center of the quartz substrate. Solid lines represent linear regressions of the data after the 10th bilayer.

linearly with salt concentration, while Decher and Lvov⁴² and others^{43,44} have observed that the growth rate increases as a square root of the salt concentration. The addition of the salt screens the electrostatic repulsion between similarly charged groups, increasing the thickness of the adsorbed polyelectrolytes. Such screening and swelling of polyelectrolyte thickness in multilayers result in additional adsorption of polymer chains to maintain the required overcharging of the surface and layer growth.⁴⁵ Quantitatively, the square root dependence of growth on salt

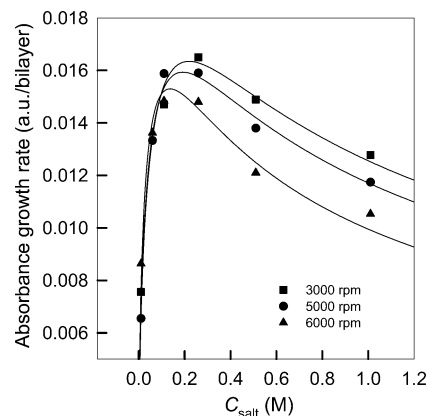


Figure 3. Dependence of the absorbance growth rate on salt concentration for multilayered films prepared with the polyelectrolyte spin assembly method at 3000 rpm (squares), 5000 rpm (circles), and 6000 rpm (triangles). The growth rate is measured at 6 mm from the center of the substrate. The solid lines are the best fit to eq 1.

concentration is predicted for quiescent (dipping) assembly at low ionic strength^{44,46} by using the Flory-type theory.²⁶ At high ionic strength ($c > 0.5$ M) Castelnovo and Joanny⁴⁷ have predicted a linear dependence on salt concentration for quiescent LbL assembly.

The second regime occurs at higher salt concentrations. In this regime, the growth rate of the polymer surface coverage decreases with increasing the salt concentration. According to our model,²⁶ and following similar work on polymer brushes,⁴⁸ in this salt concentration range the shear flow created by the rotating disc is capable of deforming the adsorbing chains and works against the electrostatic attraction between oppositely charged groups favoring chain's adsorption. It is known that polymer surface coverage in PSA exhibits significant radial dependence,²¹ due to the fact that the shear rate depends on radius in spin-coating flow. The shear rate increases linearly with the distance r from the center of the rotating disc according to an approximation close to the surface^{26,49}

$$\dot{\gamma} = \rho\omega^2rh/\eta \quad (3)$$

where η is the viscosity of the polyelectrolyte solution, ω is the angular velocity of the rotating disc, and h is the thickness of the "thinning" polymer solution. Indeed, the growth rate measured further away from the disc center (at 8 mm) for spin speed of 3000 rpm shows an even more pronounced effect of shear rate (see Supporting Information, Figure S2). In our previous study at 3000 rpm,²⁶ it was reported that the growth rates of multilayers measured by UV-vis spectroscopy and AFM showed a plateau for salt concentrations higher than 0.1 M. We note that observations in that study were made at the disk center, whereas those for Figure 3 were measured 6 mm from the disk center, a higher shear rate position (eq 3), allowing resolution of a shear flow effect at higher salt concentrations.

The radial dependence of the polymer surface coverage in multilayer coatings by PSA was followed by the PSS absorbance measured after completion of 20 deposition cycles. Such measurements are a good measure of PSA growth rate, though

(45) Ladam, G.; Schaad, P.; Voegel, J. C.; Schaaf, P.; Decher, G.; Cuisinier, F. *Langmuir* **2000**, *16* (3), 1249–1255.

(46) Losche, M.; Schmitt, J.; Decher, G.; Bouwman, W. G.; Kjaer, K. *Macromolecules* **1998**, *31* (25), 8893–8906.

(47) Castelnovo, M.; Joanny, J. F. *Langmuir* **2000**, *16* (19), 7524–7532.

(48) Harden, J. L.; Cates, M. E. *Phys. Rev. E: Stat. Phys., Plasmas, Fluids, Relat. Interdiscip. Top.* **1996**, *53* (4B), 3782–7.

(49) Alfred, G. E.; Francis, T. B.; Leslie, G. P. *J. Appl. Phys.* **1958**, *29* (5), 858–862.

(42) Lvov, Y. M.; Decher, G. *Kristallografiya* **1994**, *39* (4), 696–716.

(43) Ruths, J.; Essler, F.; Decher, G.; Riegler, H. *Langmuir* **2000**, *16* (23), 8871–8878.

(44) Steitz, R.; Leiner, V.; Siebrecht, R.; Klitzing, R. V. *Colloids Surf. A: Physicochem. Eng. Aspects* **2000**, *163* (1), 63–70.

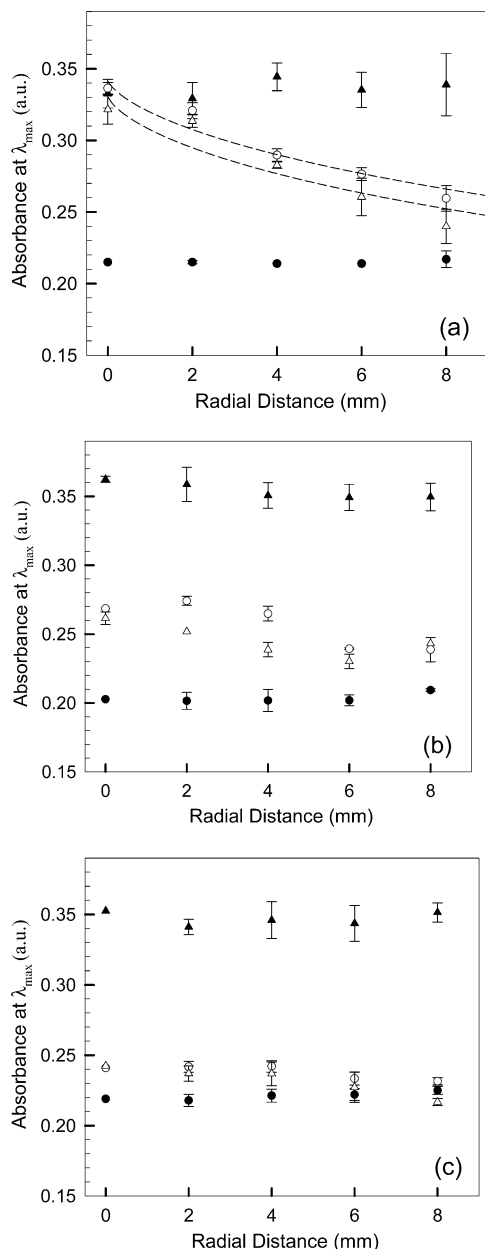


Figure 4. Radial dependence of the absorbance of PSS/PAH film at different salt concentrations: 0 M (filled circles), 0.1 M (filled triangles), 0.5 M (open circles), and 1.0 M (open triangle) at (a) 3000 rpm, (b) 5000 rpm, and (c) 6000 rpm. Each point is averaged for the four different azimuthal angles. The dashed lines in part a are the best fit to the eq 4. All measurements are taken after completion of 20 deposition cycles.

not a direct one due to the bilinear nature of multilayer growth shown in Figures 1 (inset) and 2. Figure 4 shows the radial dependence of polymer surface coverage for multilayers at different salt concentrations and spinning speeds of (a) 3000 rpm, (b) 5000 rpm, and (c) 6000 rpm. At lower salt concentrations, $c = 0$ and 0.1 M, and a spin speed of 3000 rpm (Figure 4a), the radial profile is essentially flat, suggesting a uniform polyelectrolyte surface coverage. This is another indication of the dominance of the electrostatic interactions in the low salt concentration regime. However, the growth rate of polymer surface coverage shows radial dependence for the salt concentrations of 0.5 and 1.0 M (Figure 4a), with a decrease in coverage with increasing radius. This functional form of the radial profile can be fitted by following equation obtained by substituting eq 3 in eq 1

$$\Gamma \approx \frac{\Gamma_0}{1 + \zeta(\omega^2 r)^{2/3}} \quad (4)$$

where Γ_0 and ζ are fitting parameters. However, the absorbance value at 2 mm from the disc center for the case of 0.5 and 1.0 M salt concentrations in Figure 4a, though reproducible, does not conform to this functional form. This may be due to the combined effect of higher curvature at low radius and the fairly large spot size (1 mm) used to measure absorbance in the spectrophotometer. Nevertheless, the reasonable fit of the radial data at 3000 rpm gives an indication of shear rate dominance at high salt concentrations. Such radial dependence was also observed in our previous study.²⁶ Chiarelli et al.²¹ have studied the radial dependence of the multilayer coatings assembled at 3000 rpm from salt-free solutions for weak polyelectrolyte pairs of PEI and poly[1-[4-(3-carboxy-4-hydroxyphenyl)azobenzene-sulfonamide]-1,2-ethandiy] (PAZO). They found that the film thickness, measured by ellipsometry, has weak dependence on radius, unlike the uniform coatings observed in our study from salt-free polyelectrolyte solutions. This difference might be due to the difference in charge density of the polyelectrolyte chains compared to the fully charged polyelectrolytes used in our study. As we mentioned earlier for PSA, the surface-localized shear flow may deform the adsorbed polyelectrolytes and compete with the electrostatic interactions. Thus, partially charged polyelectrolytes can have strong shear rate dependence compared to fully charged polyelectrolytes. A detailed analysis of the effect of the polyelectrolyte charge density on multilayer uniformity (radial dependence) is beyond the scope of the present study, but does warrant future attention.

Increasing the spin speed leads to stronger radial dependence. Figure 4b shows the effect of salt concentration on the radial dependence of the multilayered coatings at 5000 rpm. At low salt concentrations ($c = 0$ and 0.1 M), the variation of polymer surface coverage with radius is uniform, further confirming the dominance of the electrostatic interactions in the layer buildup. At higher salt concentration, 0.5 and 1.0 M, the radial profile is different than that seen for similar salt concentrations at 3000 rpm. Compared to Figure 4a, for radius $r < 4$ mm, the polymer surface coverage is decreased, though not as much for radial distance $r > 4$ mm. Increasing the spin speed to 6000 rpm further lowers the polymer surface coverage at smaller radii ($r < 4$ mm), producing essentially flat uniform layers at higher salt concentrations (Figure 4c). There is negligible radial dependence of the polyelectrolyte surface coverage, even for the highest studied salt concentration of 1.0 M. Thus, the decrease in polymer surface coverage with increasing spin speed is more pronounced at smaller radii. We believe that this is due to the fact that the shearing flow can stretch the polyelectrolyte chains only to a finite extent. In analogy to the case of polymer solutions⁵⁰ or tethered polymer chains⁵¹ exposed to elongational flow, there should exist a critical deformation rate beyond which the chain has fully extended conformation on surface, thus showing no further effect of shear rate on the coatings. The shear rate in PSA depends on the spin speed and radius according to eq 2. For multilayers assembled at 5000 rpm, such critical shear rate is apparently achieved at radius $r \approx 4$ mm. On increasing the spin speed, the critical shear rate, corresponding to full extension of the polyelectrolyte chains, is achieved at smaller radial distance (see eq 4), as seen by the decrease in absorbance at lower radius for films assembled at 6000 rpm (Figure 4c). This eventually leads to a planarized

(50) Larson, R. G. *J. Rheol.* **2005**, *49* (1), 1–70.

(51) Perkins, T. T.; Smith, D. E.; Larson, R. G.; Chu, S. *Science* **1995**, *268* (5207), 83–87.

coating, as observed for higher shear rate and salt concentrations. The conventional spin-coating method of the uncharged polymers has been shown to produce such highly planarized coatings.^{52–54} Thus, the shear stress affects the adsorbed polyelectrolyte chains' conformations and thereby affects the surface coverage and growth rate.

In the light of the effects described above, we reasoned that the impact of shear stress on polyelectrolyte adsorption may be nonlocal and impact the surface morphology. Thus, contact-mode AFM was used to investigate the effect of the spin speed and salt concentration on the surface morphology, roughness, and thickness of the multilayered coatings. The data were collected after completion of 32 deposition cycles at a radius of 6 mm from the disk center. We found that the roughness of the multilayer coatings increases monotonically with the salt concentration at a fixed spin speed, unlike the nonmonotonic behavior observed for the growth rate of the same multilayered coatings. Figure 5 shows the surface topography obtained by AFM at different salt concentrations (a) 0 M, (b) 0.1 M, and (c) 1.0 M and at the spin rate of 5000 rpm. The PSA multilayer coatings deposited from salt-free solutions are very smooth, with a root-mean-square (rms) roughness value equal to 1.31 nm. As the salt concentration is increased to 0.1 M, the surface roughness increases (Figure 5b), with a rms roughness at this salt concentration tripling to 3.94 nm. Upon further increasing salt concentration to 1.0 M (Figure 5c), the rms roughness increases ~ 10 times, compared to the multilayers assembled from salt-free solution, to 10.12 nm. A similar increase in the roughness of multilayered coatings with increasing ionic strength has been observed with AFM studies of dipping assembly^{55,56} and for the PSA at 3000 rpm.²⁶ In a previous study of dipping LbL assembly,⁵⁵ wormlike (or "vermiculate") patterns were observed for those coatings deposited from solutions with 1.0 M NaCl concentration. Those features were ~ 50 nm in height, 200 nm in width, and had rms roughness of ~ 20 nm. In the present study, for PSA at 5000 rpm and 1.0 M NaCl concentration (Figure 5c), the features are ~ 40 nm in height, ~ 450 nm in width, and with a much lower rms roughness of ~ 10 nm. Thus, the spinning of the substrate produces features that are broader and flattened as compared to the films obtained quiescently at the same solution ionic strengths.

These characteristic features become less pronounced at higher spin speeds. The multilayered coatings spin-coated at 6000 rpm and salt concentration of 1.0 M have features ~ 15 nm in height and ~ 350 nm in width with mean square roughness of around 7 nm (see Supporting Information, Figure S3). It is known that an increase in the salt concentration increases the characteristic features sizes.⁵⁵ Shear tends to flatten out the features, increasingly at higher spin speeds. These characteristic features of the multilayered coatings at high salt concentrations might give an additional clue in understanding the construction of the multilayered coatings under the effect of shear flow.

In order to quantify for the AFM measurements, the height-histogram analysis was employed. Figure 6 shows the film height distribution function obtained from AFM images taken for the multilayered coatings at different salt concentrations at 5000 rpm. We observe that coating roughness increases with increasing salt concentration, as indicated by the increase of the width of the height distribution functions. The height distribution function

(52) Stillwagon, L. E.; Larson, R. G.; Taylor, G. N. *J. Electrochem. Soc.* **1987**, 134 (8A), 2030–2037.

(53) Stillwagon, L. E.; Larson, R. G. *J. Appl. Phys.* **1988**, 63 (11), 5251–5258.

(54) Stillwagon, L. E.; Larson, R. G. *Phys. Fluids A* **1990**, 2 (11), 1937–1944.

(55) McAloney, R. A.; Sinyor, M.; Dudnik, V.; Goh, M. C. *Langmuir* **2001**, 17 (21), 6655–6663.

(56) Dubas, S. T.; Schlenoff, J. B. *Langmuir* **2001**, 17 (25), 7725–7727.

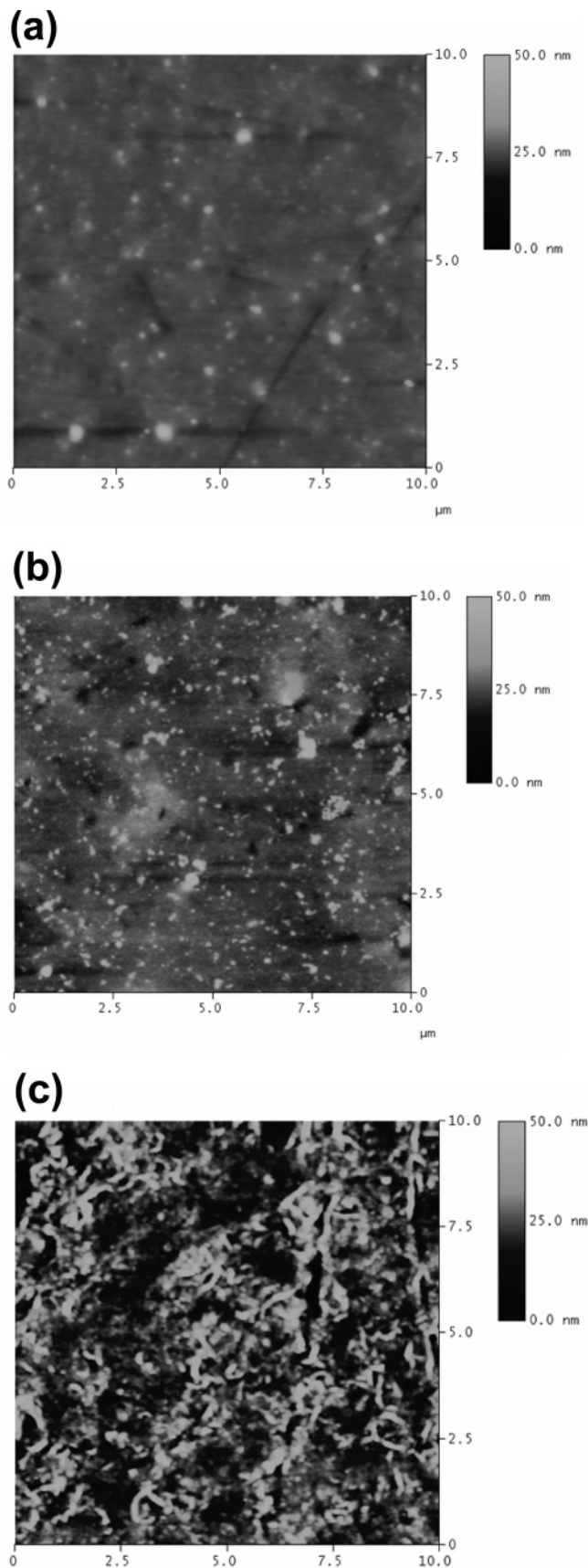


Figure 5. Dependence of the roughness of PSS/PAH films on salt concentration at 5000 rpm. AFM measurements are taken at 6 mm from the center of the disk after completion of 32 deposition cycles at different salt concentrations: (a) 0 M, (b) 0.1 M, and (c) 1 M.

for coatings deposited from solutions with salt concentration 1.0 M was very broad, indicating a rough coating compared to the

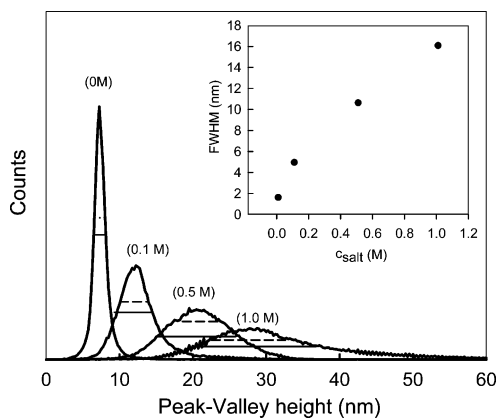


Figure 6. Peak–valley height distribution functions measured from the AFM images at 5000 rpm and different salt concentrations. The width of the solid line is the full width at half-maximum (fwhm) and the dashed line represents the width of the rms roughness. The inset shows the fwhm at different salt concentrations.

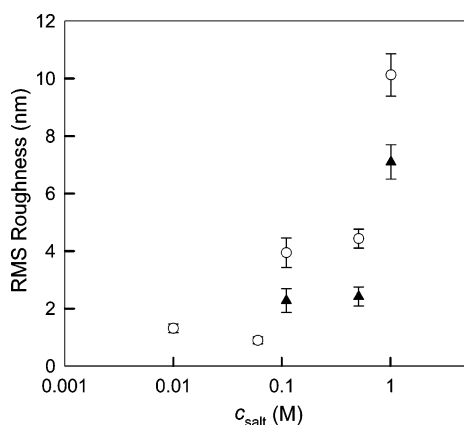


Figure 7. Dependence of film roughness on the salt concentration after completion of 32 deposition cycles of (PSS/PAH)₃₂ at ($c_p = 10^{-2}$ M, pH 3.5) for 5000 rpm (circles) and 6000 rpm (triangles).

narrow distribution for films assembled from salt-free solutions (0 M) at the same spin rate. The width of the peak at the half-maximum height is shown by the solid lines in Figure 6 and plotted in the inset, while the dashed horizontal lines represent the rms roughness. The inset indicates that the coating roughness increases almost linearly with the salt concentration, which is in agreement with the previous studies for the dipping⁵⁵ and PSA²⁶ at 3000 rpm.

The dependence of rms roughness (eq 2) on ionic strength is plotted in Figure 7. This figure shows that the roughness of coatings made at a higher spin rate (6000 rpm) is significantly lower than that for coatings assembled at 5000 rpm for all salt concentrations. Furthermore, the rms roughness increases sharply at the salt concentration above 0.5 M for both spin speeds of 5000 and 6000 rpm, as seen in Figure 7. On comparison, the roughness values of the multilayered coatings obtained by dipping⁵⁵ and by PSA at 3000 rpm²⁶ are higher than those values achieved for spin speeds of 5000 and 6000 rpm in the present study. Given the findings on growth rate dependence as influenced by the combined effects of added salt and shear flow, we reason that the observed decrease in the coating roughness is a manifestation of the shear flow impact on chain conformations and larger scale of the adsorption structures.

Finally, AFM was used in a profilometric manner to quantify the thickness of the multilayers by PSA to confirm the existence of the two regimes as predicted by our model and as witnessed

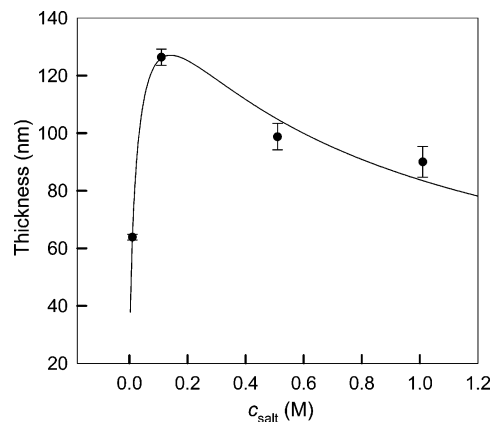


Figure 8. Thickness of the PSS/PAH multilayer coatings at 6 mm from the center of the substrate after deposition of 32 bilayers at 6000 rpm. The solid line is the fit to the eq 2.

using UV–vis absorption measurements (Figures 1 and 2). As one example, Figure 8 shows AFM-measured thicknesses for multilayered coatings after completion of the 32 deposition cycles from PSS/PAH solutions at 6000 rpm and different salt concentrations. The measured film thickness features a non-monotonic dependence on salt concentration similar to one obtained for polymer surface coverage by UV–vis measurements (see Figure 3). The thickness increases with increasing salt concentration for the range of salt concentrations below 0.1 M and then decreases at higher salt concentrations 0.5 and 1.0 M. The salt concentration dependence of the film thickness is also in a good agreement with the predictions of the scaling model of Lefaux et al.,²⁶ as given by eq 1, thus confirming the existence of the two regimes of electrostatic dominance at lower salt concentration and shear dominance at high salt concentration.

Conclusions

We have studied the combined effect of spin speed and salt concentration on the growth, morphology, thickness, and roughness of the multilayer coatings made by sequential spin coating from polyelectrolyte solutions, termed polyelectrolyte spin assembly. The growth of the multilayered coatings shows a nonmonotonic dependence on ionic strength, first increasing and then decreasing with increasing solution ionic strength. We conclude that this behavior is a manifestation of two competing mechanisms for the multilayer assembly process, electrostatic interactions dominating film growth at low ionic strengths and shear flow dominating at high ionic strengths. This can be explained in the framework of the Flory-type theory²⁶ of the multilayer adsorption that takes into account the formation of the ionic pairs between oppositely charged chains and chain deformation in the external shear flow created by a rotating disc. The scaling equation fits our experimental data for the growth of the multilayer surface coverage and multilayer thickness at the multilayer at different spin speeds reasonably well. Additionally, while the multilayered coatings do not show a radial dependence, for the multilayers made at low salt concentrations below 0.1 M, independent of spin speed, a strong radial dependence was observed at higher ionic strengths, with coverage decreasing radially. This radial dependence of polymer surface coverage, in good agreement with our model for PSA, is concluded to be due to the linear increase of the local shear rate with distance r from the disc center. However, further increase of the spin speed to 6000 rpm leads to planarization of the film and almost uniform polymer surface coverage over the entire disc. It is argued that the influence of shear is bounded, perhaps by full chain

extension. Topographically, the multilayered coatings are smooth and featureless at low salt concentrations with dimensions of the characteristic features evolving as the ionic strength of the polyelectrolyte solution is increased. The dimensions of these features are less pronounced for the multilayers formed by the spin-assembly than quiescent adsorption at the same salt concentrations. The feature size of the multilayered coatings at high ionic strength decreases upon increasing the spin speed, further confirming the effect of the shear rate on the chain conformations. Thus, the variations in salt concentration and the spin rate are two parameters that allow control over the growth rate and film thickness during multilayer assembly by the spin-coating method.

Acknowledgment. Authors thank Prof. Clemens Burda for allowing use of the UV–vis spectrophotometer with focused spot size in this study. Financial support from Ivoclar-Vivadent (P.T.M.) and NSF/DMR (A.V.D.) is acknowledged.

Supporting Information Available: (1) growth of PSS/PAH multilayers by PSA process up to 50 bilayers indicating steady-state multilayer growth, (2) growth rate of multilayers by PSA at 3000 rpm at different radial distance, and (3) roughness at different salt concentrations of multilayers by PSA at 6000 rpm. This material is available free of charge via the Internet at <http://pubs.acs.org>.

LA7020676